Supplemental materials

The negative elongation factor (NELF) is required for the maintenance of proviral latency but does not induce promoter proximal pausing of RNAP II on the HIV LTR

Julie K. Jadlowsky[a,b], Julian Y. Wong[a], Amy C. Graham[a], Curtis Dobrowolski[a], Renee L. Devor[a,c], Mark D. Adams[a,d], Koh Fujinaga[a,e] & Jonathan Karn[a]

[a]Department of Molecular Biology and Microbiology, Case Western Reserve University School of Medicine, Cleveland, Ohio 44106

[b]Translational Research Program, Perelman School of Medicine, University of Pennsylvania, Philadelphia, Pennsylvania 19104

[c]Department of Pediatrics, University of Toledo, Toledo Ohio, 43614

[d]The J Craig Venter Institute, San Diego, California, 92037

[e]Departments of Medicine, Microbiology and Immunology, Rosalind Russell Research Center, University of California, San Francisco, San Francisco, California, 94143

Address correspondence to Jonathan Karn, jonathan.karn@case.edu.

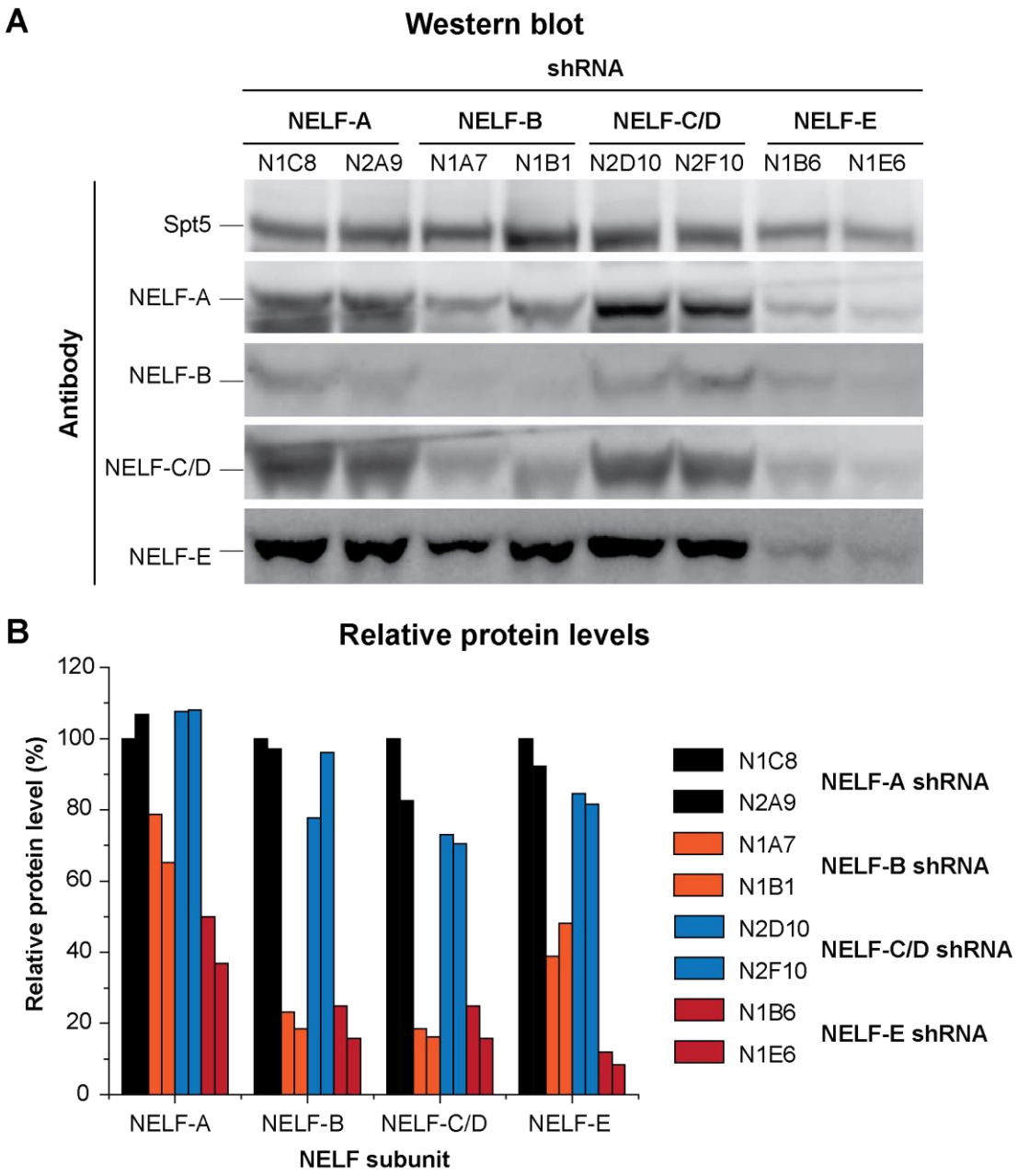

FIG S1 Western blot analysis of NELF subunit expression. (A) Blot of individual clones of E4 cells superinfected with shRNA-expressing lentiviral vectors to individual NELF subunits. Samples from left to right: NELF-A (NIC8, N2A9). NELF-B (N1A7, N1B1), NELF-C/D (N2D10, N2F10), NELF-E (N1B6, N1E6). Nuclear extracts from each cell line were prepared, fractionated by 10% SDS-PAGE and blotted against the following primary antibodies: NELF-E, NELF-A, Spt5 (Santa Cruz Biotechnology), Cobra (NELF B) (Bethyl Laboratories), THP1 (NELF C/D) (Acris Antibodies). Horseradish peroxidase (HRP)-conjugated secondary antibodies (Dako) were used along with ECL Western Blotting Detection Reagents (GE Healthcare) to detect proteins by chemiluminescence using the ImageQuant LAS 4000. (B) Quantitative analysis of the western blot in panel A. Gel band intensity was measured by using ImageQuant TL (GE Healthcare). Relative protein levels were normalized to the signal intensity of the Spt5 loading control and plotted. Note that significant knockdown of all the NELF subunits was achieved using shRNAs to NELF-E and NELF-B but there was relatively little knockdown using the NELF-A and NELF-C/D shRNAs.

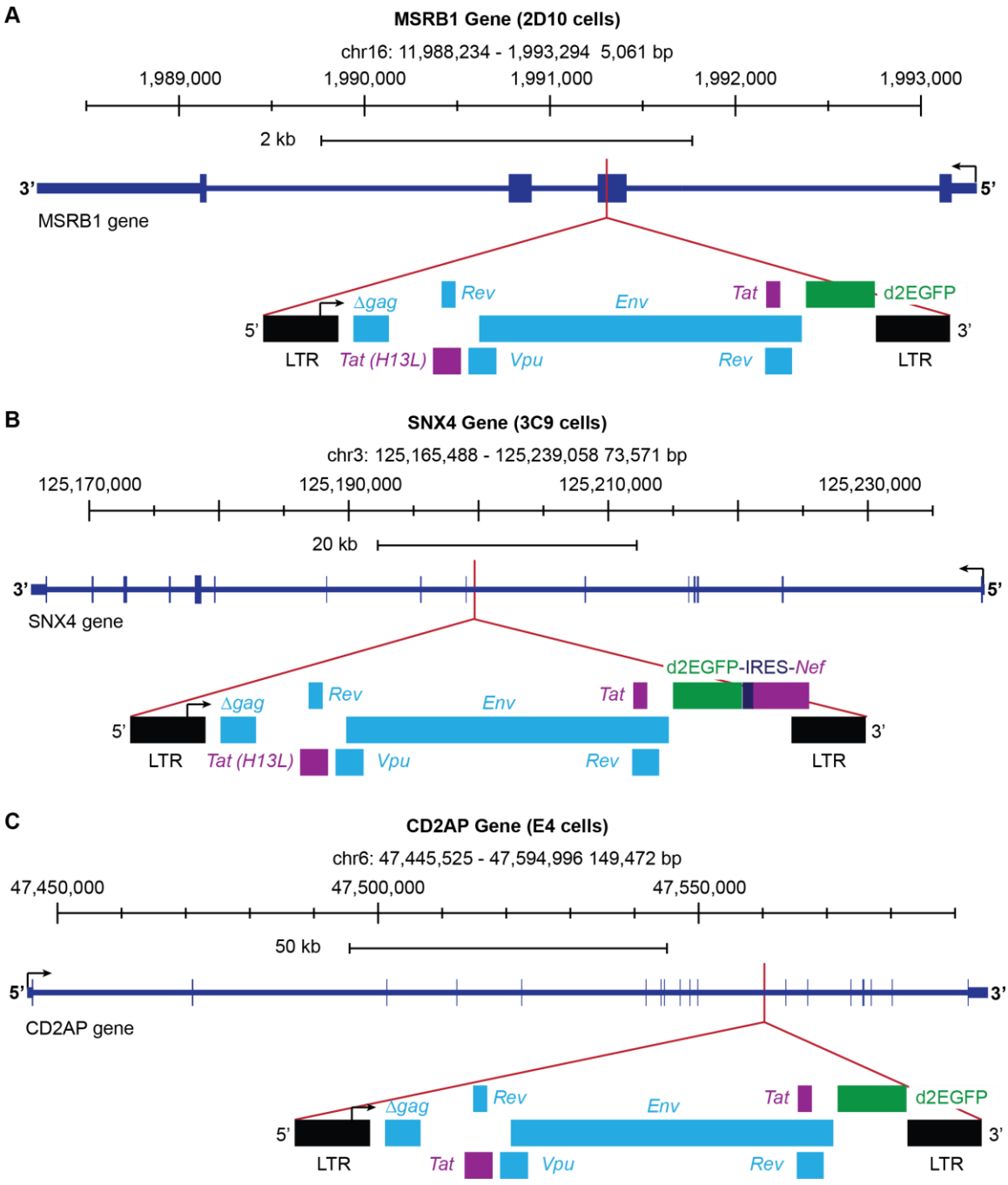

FIG S2 Location of proviral integration sites and orientation of the proviral vector. (A) MSRB1 gene which carries the provirus from 2D10 cells. This provirus encodes the Tat H13L mutation. (B) SNX4 gene, which carries the provirus from 3C9 cells. This provirus encodes a d2EGFP-IRES-Nef translation unit. (C) CD2AP gene, which the provirus in E4 cells. This provirus carries a wildtype Tat gene. Note that we have corrected the location for the provirus in E4 cells which was previously erroneously mapped (Friedman et al., 2011; Pearson et al., 2008). For the gene diagrams thin bars represent the introns, thick bars the exons and medium bars represent non-coding exon sequences.

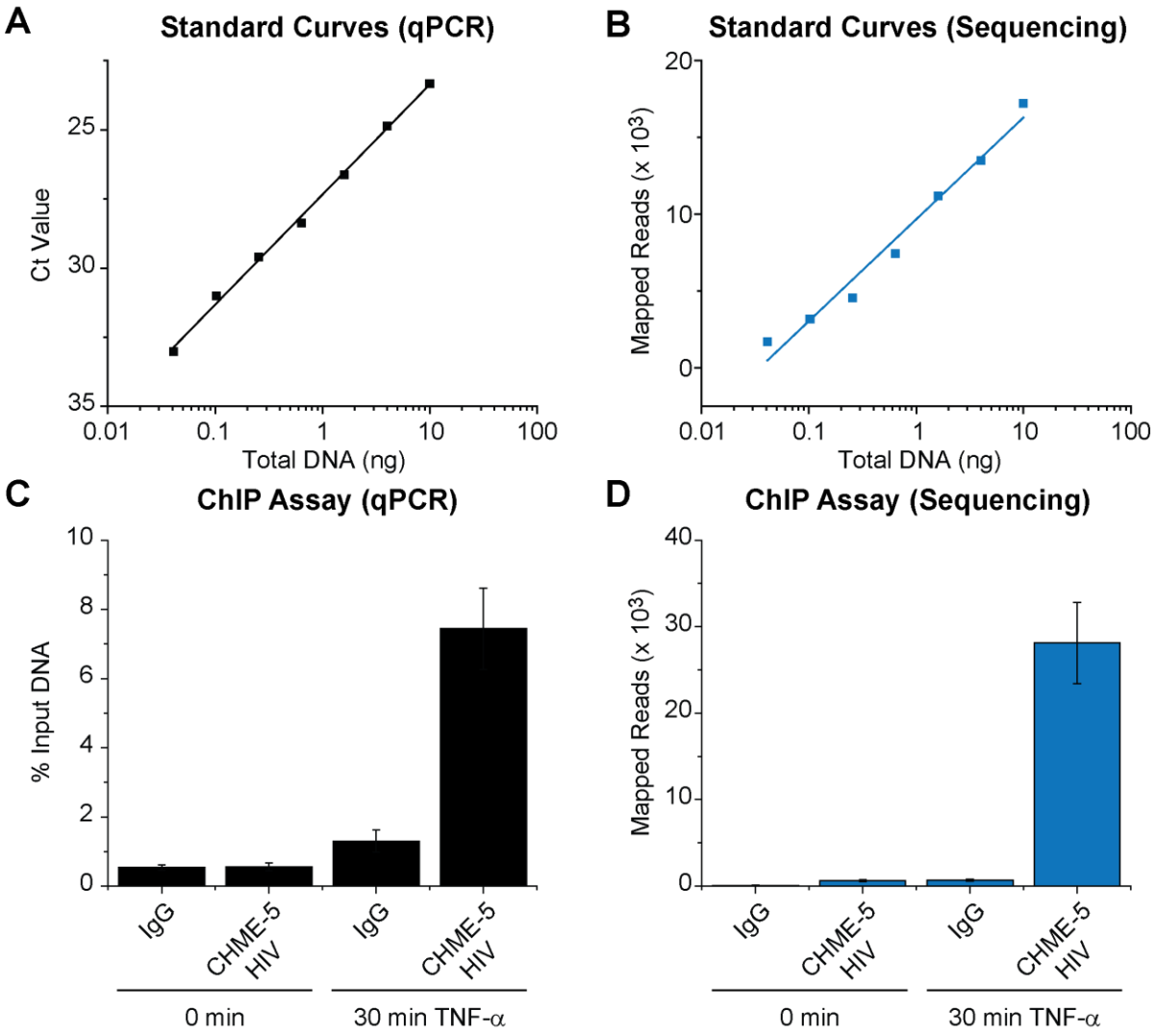

FIG S3 Comparison of ChIP assay results obtained by qPCR and Ion Torrent sequencing. (A) Standard curve for qPCR assay. DNA from Jurkat cells was serially diluted and 7 aliquots between 0.003 ng and 15 ng were amplified using the primers to Nuc-0 (-390 F, ACA CAC AAG GCT ACT TCC CTGA, and -283 R, TCT ACC TTA TCT GGC TCA ACT GGT). PCR amplifications were performed in 25 µl reaction mixtures containing 5 µl of DNA, 12.5 µl of SYBR green master mix (Roche), and 1 µl of each primer using real-time qPCR (BioRad). Plot shows Threshold Ct values verses input DNA concentrations. (B) PCR products for sequencing were produced using the same method and serial dilution as described above with the addition of a barcoded adapter to each primer sequence. Samples were pooled and 300pg of DNA was used for quantification by Ion Torrent sequencing. The number of reads mapping to the amplified sequence was plotted against input DNA concentrations. (C) RNAP II levels at the Nuc-1 region (+ 30 F-CTGGGAGCTCTCTGGCTAACT A, HIV +134 R-TTA CCA GAG TCA CAC AAC AGA CG) of the HIV LTR in latently infected CHME5 (microglial) cells (Wires et al., 2012). Cells were either uninduced or induced for 30 with 10 ng/ml TNF-α. The DNA amounts of the amplified PCR products were measured by real-time qPCR. Percentage input was determined by comparing the Ct value of each sample to a standard curve generated from a serial dilution of genomic input DNA. For each condition, a non-specific IgG antibody was included as a background control. (D) Analysis of ChIP samples by Ion Torrent Sequencing. The same samples in panel C were produced using the same PCR method as described above and were barcoded, pooled, and 300pg of DNA was analyzed by direct sequencing and the number of mapped reads is plotted. Note that there is a strongly reduced background in the sequenced samples.

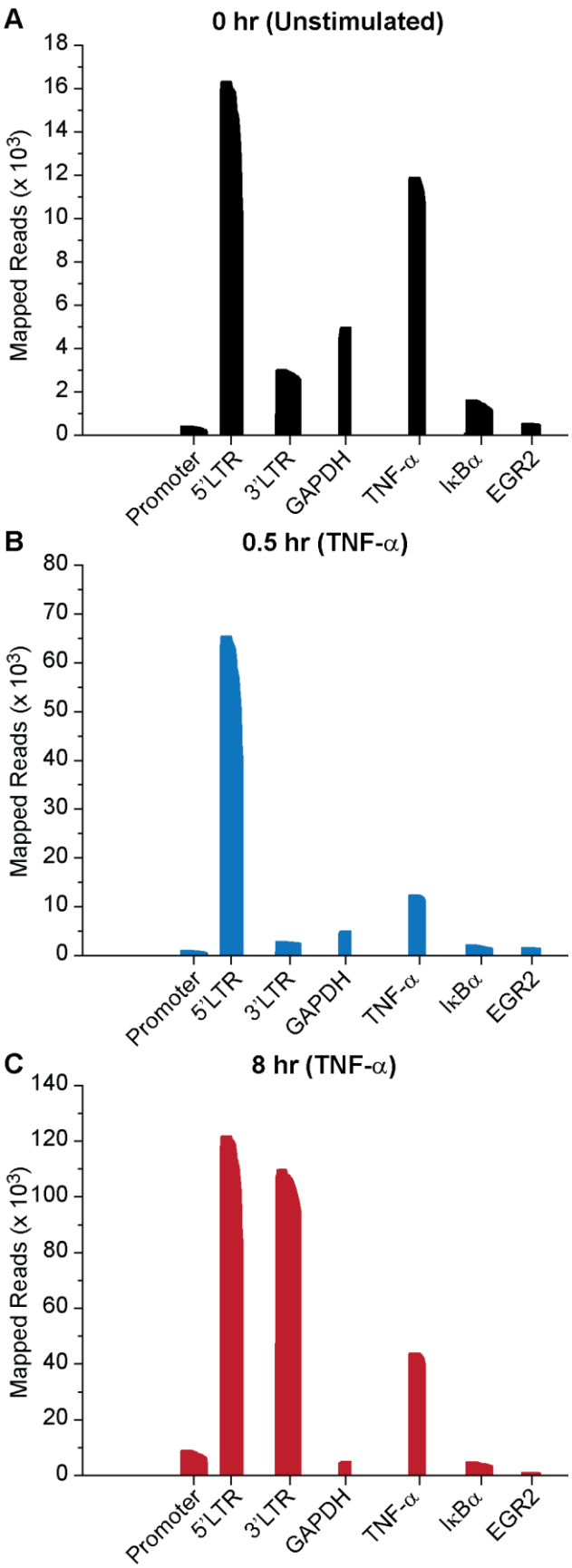

FIG S4 Induction of RNAP II accumulation at the HIV LTR following TNF-α stimulation. and the RNAP II levels at multiple sites on the proviral LTR and cellular genes was measured by ChIP assays. (A) Unstimulated E4 cells . (B) E4 cells stimulated for 0.5 hr 10 ng/ml TNF-α. (C) E4 cells stimulated for 8 hrs with 10 ng/ml TNF-α. Sequencing reads were mapped to a synthetic template carrying 200 bp fragments surrounding the anticipated PCR product sequences. Individual PCR reactions using bar-coded primers were performed for each activation condition in 96 well plates. The amplifications were monitored by real-time qPCR and stopped at mid-log phage. The PCR samples were pooled prior to sequencing. Primers used were the HIV promoter HIV (-116 F-AGC TTG CTA CAA GGG ACT TTC C, HIV + 4 R-ACC CAG TAC AGG CAA AAA GCA G), the 5' and 3' LTR specific primers (Table 1) and primers to the following cellular genes: glyceraldehyde 3-phosphate dehydrogenase (GAPDH) gene (+492 F-TGA GCA GAC CGG TGT CAC TA, +348 R-AGG ACT TTG GGA ACG ACT GA), IκBα (+155 F-AAG AAG GAG CGG CTA CTG GAC; +237 R-TCC TTG ACC ATC TGC TCG TAC T), TNF-α (+584 F- AAG GAC ACC ATG AGC ACT GAA A; +683 R-GAG AAG AGG CTG AGG AAC AAG C) and EGR2 (+35 F-CGA GGG GAC TCA CTG ACT GTT A; +126 R-TTG CCA CTG ACT CTC TCC TGT C). Plots show the number of mapped reads. Note the slight tailing off of the reads on the 5' ends due to incomplete sequencing of specific PCR products.

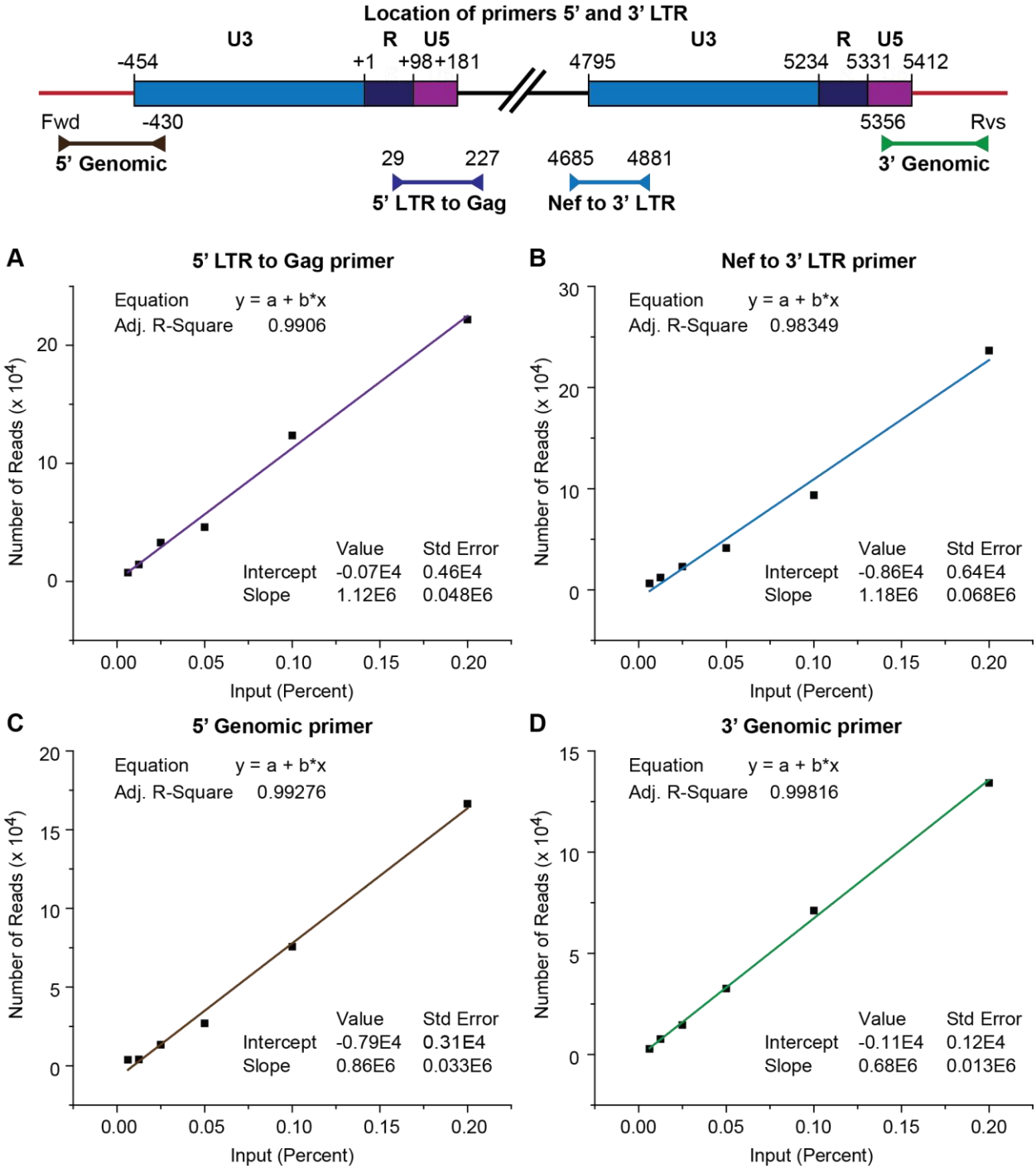

FIG S5 Standard curve for Ion Torrent Sequencing assay. Top: Location of primers used for ChIP assays (see Table 2 for primer sequences). Fwd: Forward genomic primer. Rvs: Reverse genomic primer. DNA from the E4 Jurkat cell line was serially diluted and 7 aliquots containing DNA ranging between 0.003 ng and 15 ng were amplified using the indicated primers. (A) 5' LTR to Gag primer pair. (B) Nef to 3' LTR primer pair. (C) 5' flanking genomic primer to 5' LTR primer pair. (D) 3' LTR to 3' flanking genomic primer pair.

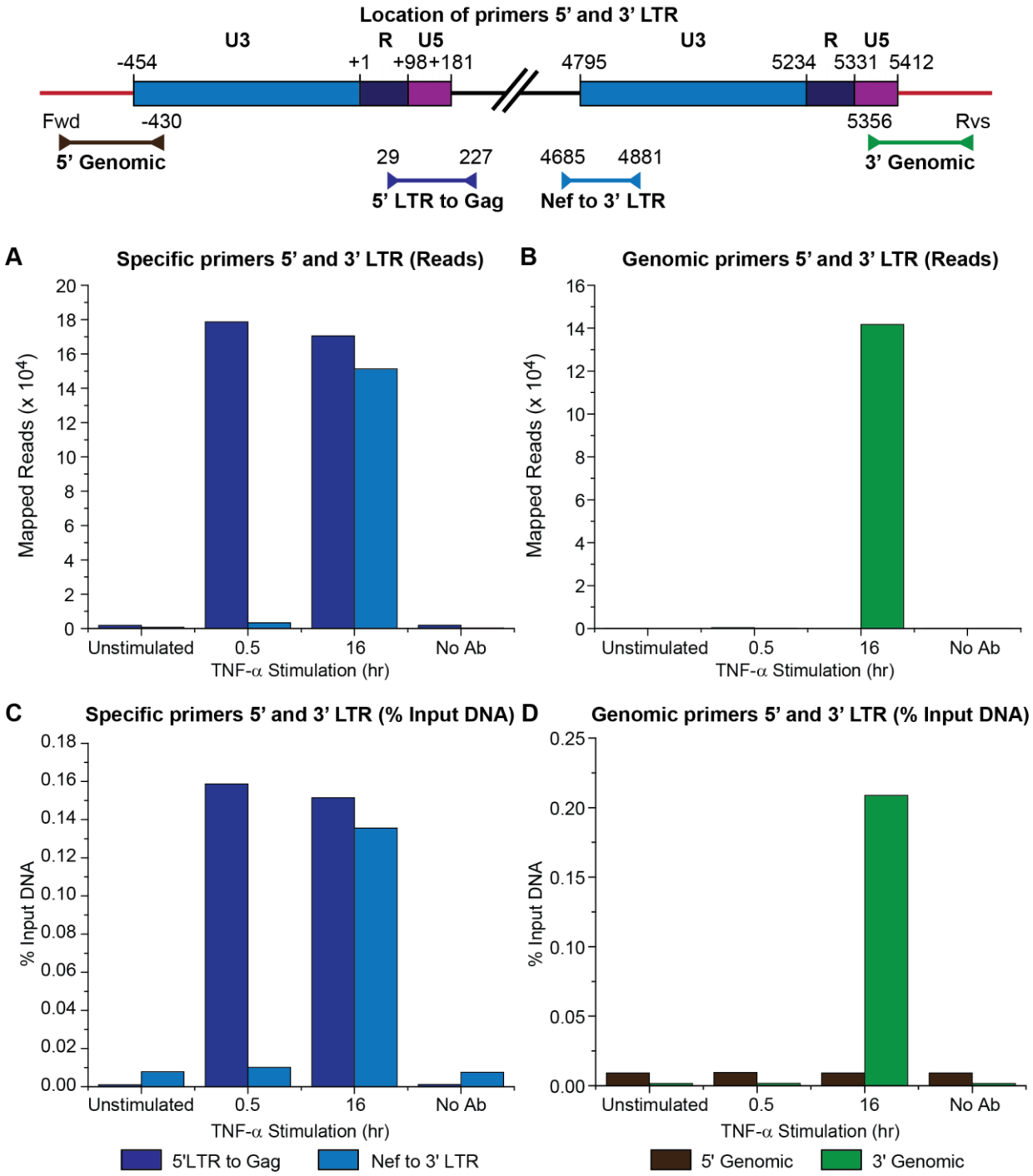

FIG S6 RNAP II accumulates on the 5' LTR but not on the 3' LTR in latently infected E4 cells. Top: Schematic diagram showing the location of primers used for ChIP assays (see Table 2 for primer sequences). Fwd: Forward genomic primer. Rvs: Reverse genomic primer. (A) ChIP analysis of RNAP II levels on the 5' and 3' proviral LTR using LTR-specific primers. Analysis was performed on E4 cells induced for 0, 0.5 or 16 hrs with 2 ng/ml TNF-α. Data is expressed as sequenced reads. (B) Analysis of the same samples as panel B using genomic primers. (C) Data from panel A converted to % input DNA based on the standard curves presented in Fig S5. Note that background values are increased due to the non-linearity of the readout at very low DNA levels. (D) Data from panel B converted to % input DNA based on the standard curves presented in Fig S5.

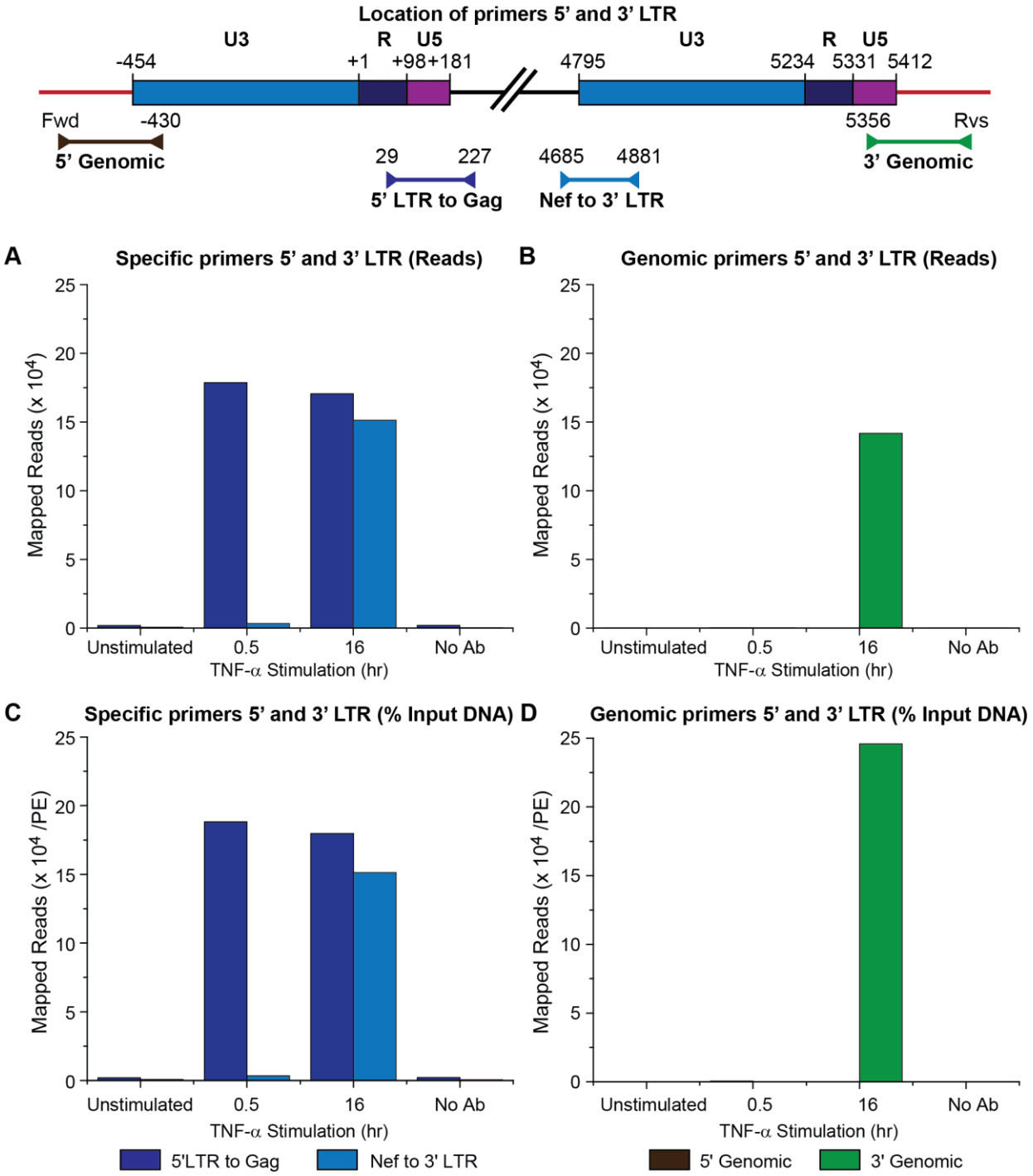

FIG S7 RNAP II accumulates on the 5' LTR but not on the 3' LTR in latently infected E4 cells. Top: Schematic diagram showing the location of primers used for ChIP assays (see Table 2 for primer sequences). Fwd: Forward genomic primer. Rvs: Reverse genomic primer. (A) ChIP analysis of RNAP II levels on the 5' and 3' proviral LTR using LTR-specific primers. Analysis was performed on E4 cells induced for 0, 0.5 or 16 hrs with 2 ng/ml TNF-α. Data is expressed as sequenced reads. (B) Analysis of the same samples as panel B using genomic primers. (C) Data from panel A corrected for relative primer efficiency (PE = the normalized slopes of the standard curves presented in Fig S5). (D) Data from panel B corrected for relative primer efficiency.

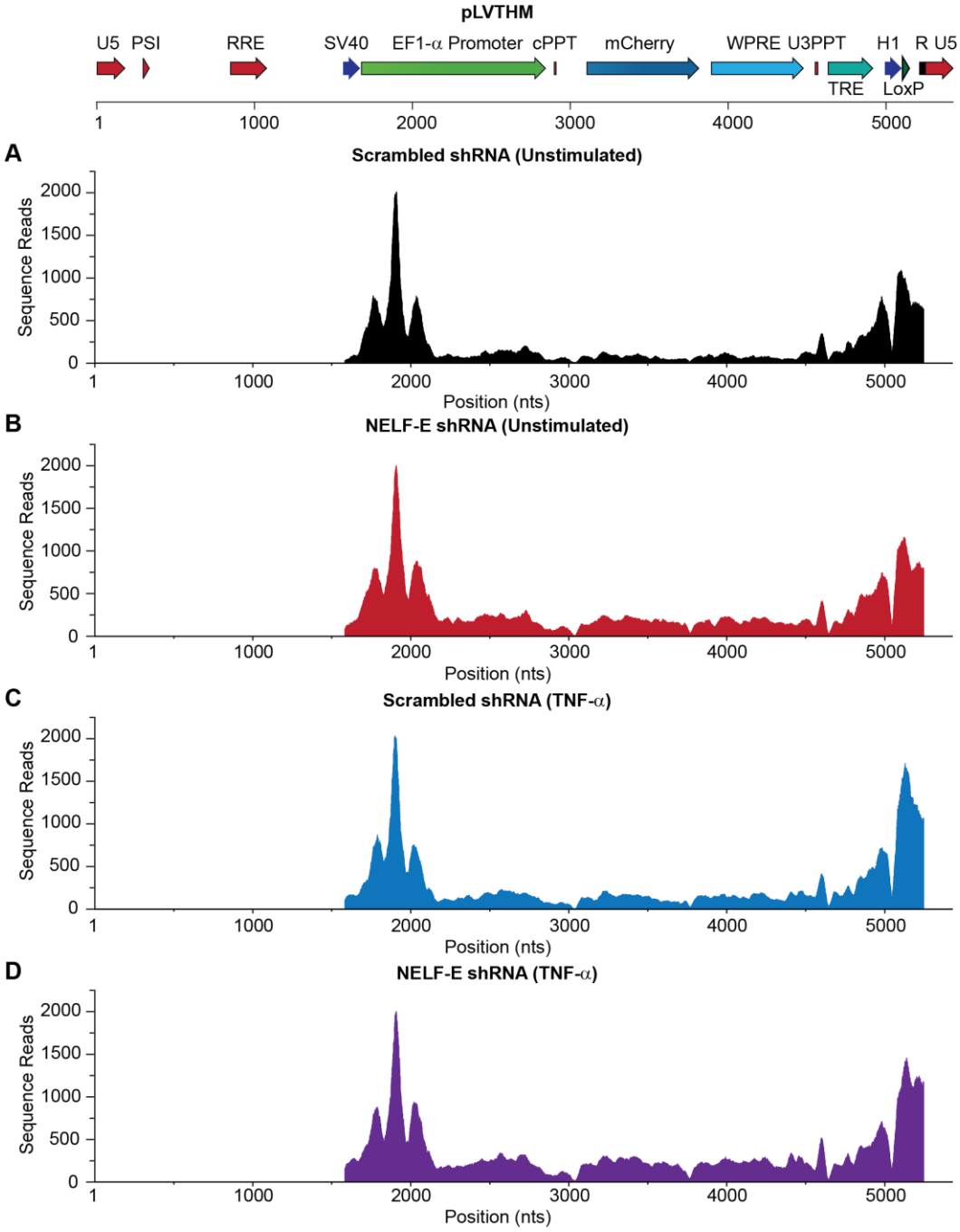

FIG S8. The distribution of RNA polymerase on the pLVTHM vector for delivery of shRNA. ChIP-Seq assays performed using the parental line E4 and clones carrying the NELF-E shRNA (N1C6) and its scrambled control (N1D9). (A) Unstimulated control (N1D9) cells. (B) Control cells stimulated with 10 ng/ml TNF-α for 60 min. (C) Unstimulated NELF-E shRNA (N1C6) cells. (D) NELF-E shRNA cells activated by 10 ng/ml TNF-α for 60 min. Note that the internal EF1-α promoter encoded by the vector is only weakly stimulated by NELF knockdown or TNF-α activation. Reads were only mapped to unique sequences in the vector and not to regions derived from the HIV proviruses. The HIV LTR is inactivated in this vector due to deletion of the U3 region.

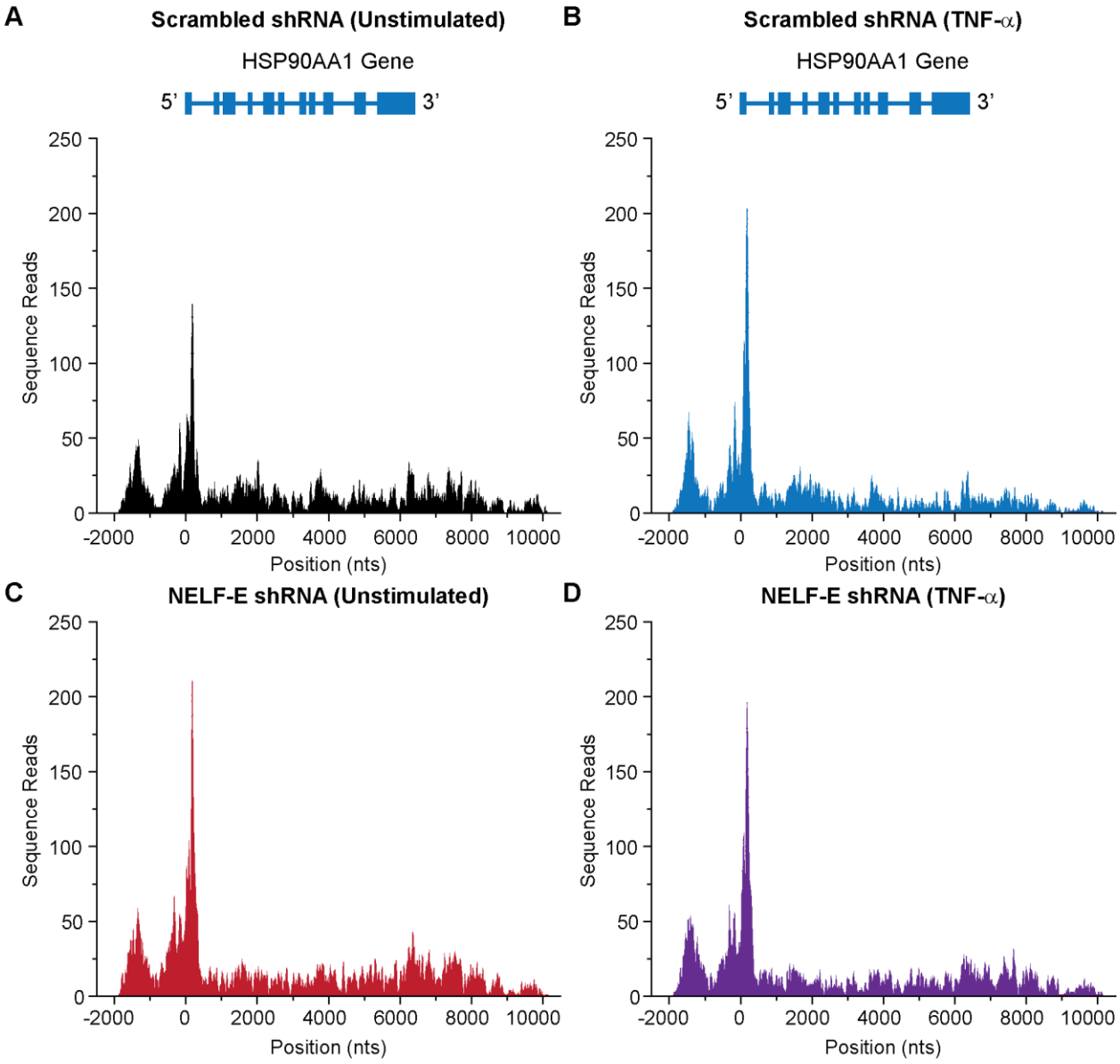

FIG S9 The distribution of RNA polymerase on the HSP90AA1 Gene. ChIP-Seq assays performed using the parental line E4 and clones carrying the NELF-E shRNA (N1C6) and its scrambled control (N1D9). (A) Unstimulated control (N1D9) cells. (B) Control cells stimulated with 10 ng/ml TNF-α for 60 min. (C) Unstimulated NELF-E shRNA (N1C6) cells. (D) NELF-E shRNA cells activated by 10 ng/ml TNF-α for 60 min. Note that the HSP90AA1 gene is an example of a gene that is weakly stimulated by NELF knockdown and insensitive to TNF-α.

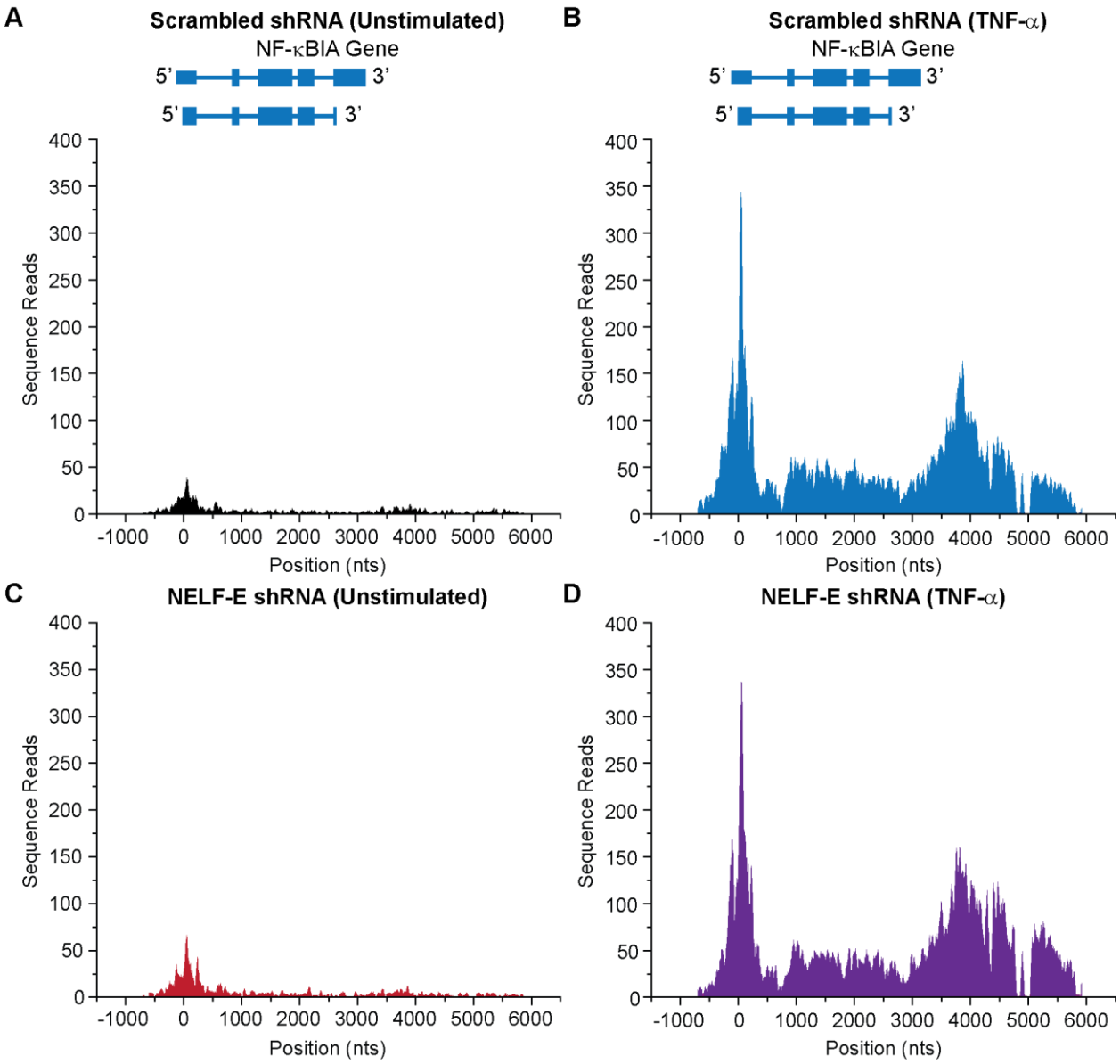

FIG S10 The distribution of RNA polymerase on the NF-κBIA Gene was measured by ChIP-Seq assays performed using the parental line E4 and clones carrying the NELF-E shRNA (N1C6) and its scrambled control (N1D9). (A) Unstimulated control (N1D9) cells. (B) Control cells stimulated with 10 ng/ml TNF-α for 60 min. (C) Unstimulated NELF-E shRNA (N1C6) cells. (D) NELF-E shRNA cells activated by 10 ng/ml TNF-α for 60 min. Note that the NF-κBIA Gene is an example of a gene that is weakly stimulated by NELF knockdown but highly responsive to TNF-α.

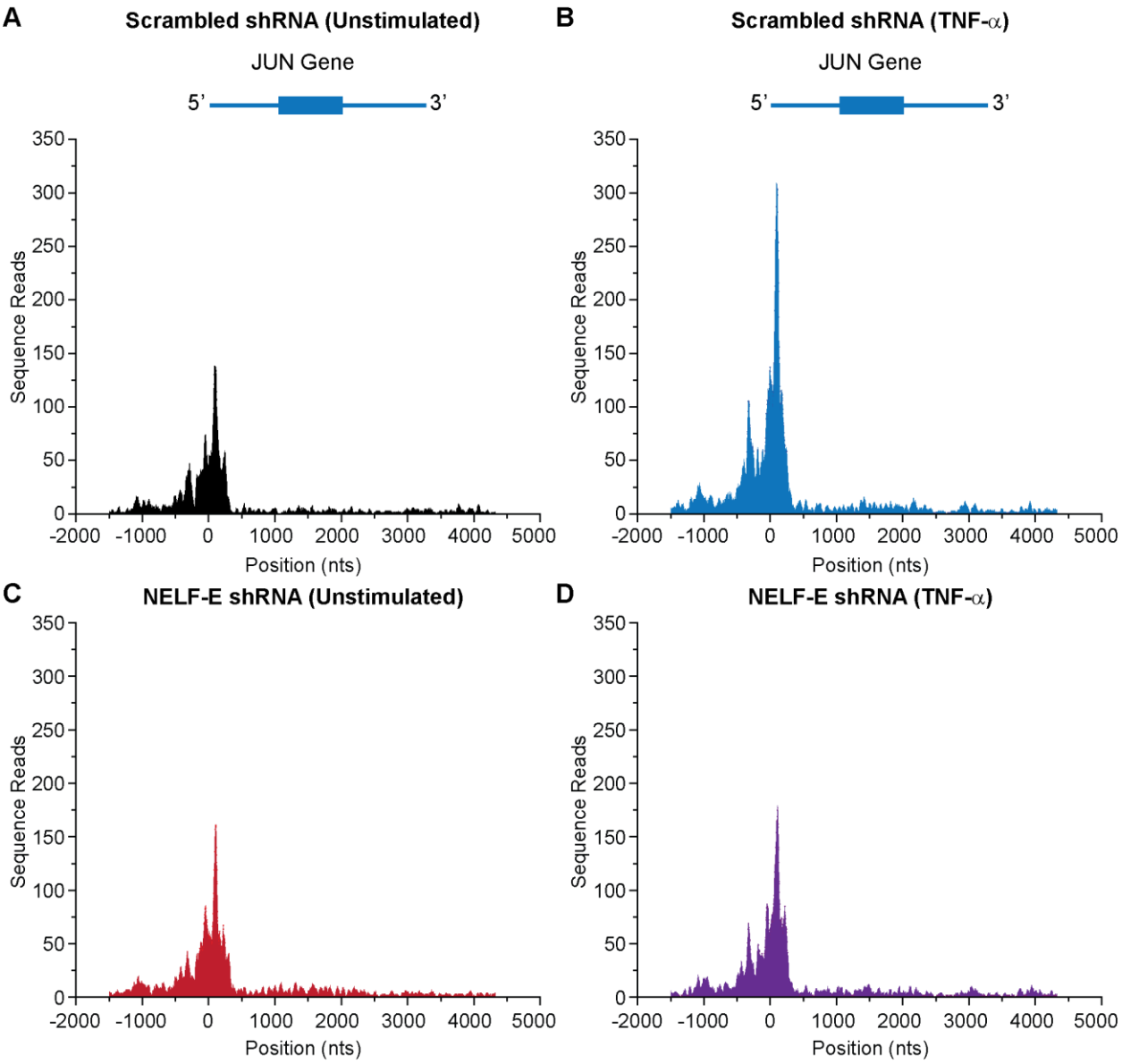

FIG S11 The distribution of RNA polymerase on the JUN Gene was measured by ChIP-Seq assays performed using the parental line E4 and clones carrying the NELF-E shRNA (N1C6) and its scrambled control (N1D9). (A) Unstimulated control (N1D9) cells. (B) Control cells stimulated with 10 ng/ml TNF-α for 60 min. (C) Unstimulated NELF-E shRNA (N1C6) cells. (D) NELF-E shRNA cells activated by 10 ng/ml TNF-α for 60 min. Note that the JUN Gene is an example of a gene that is weakly stimulated by NELF knockdown but highly responsive to TNF-α.

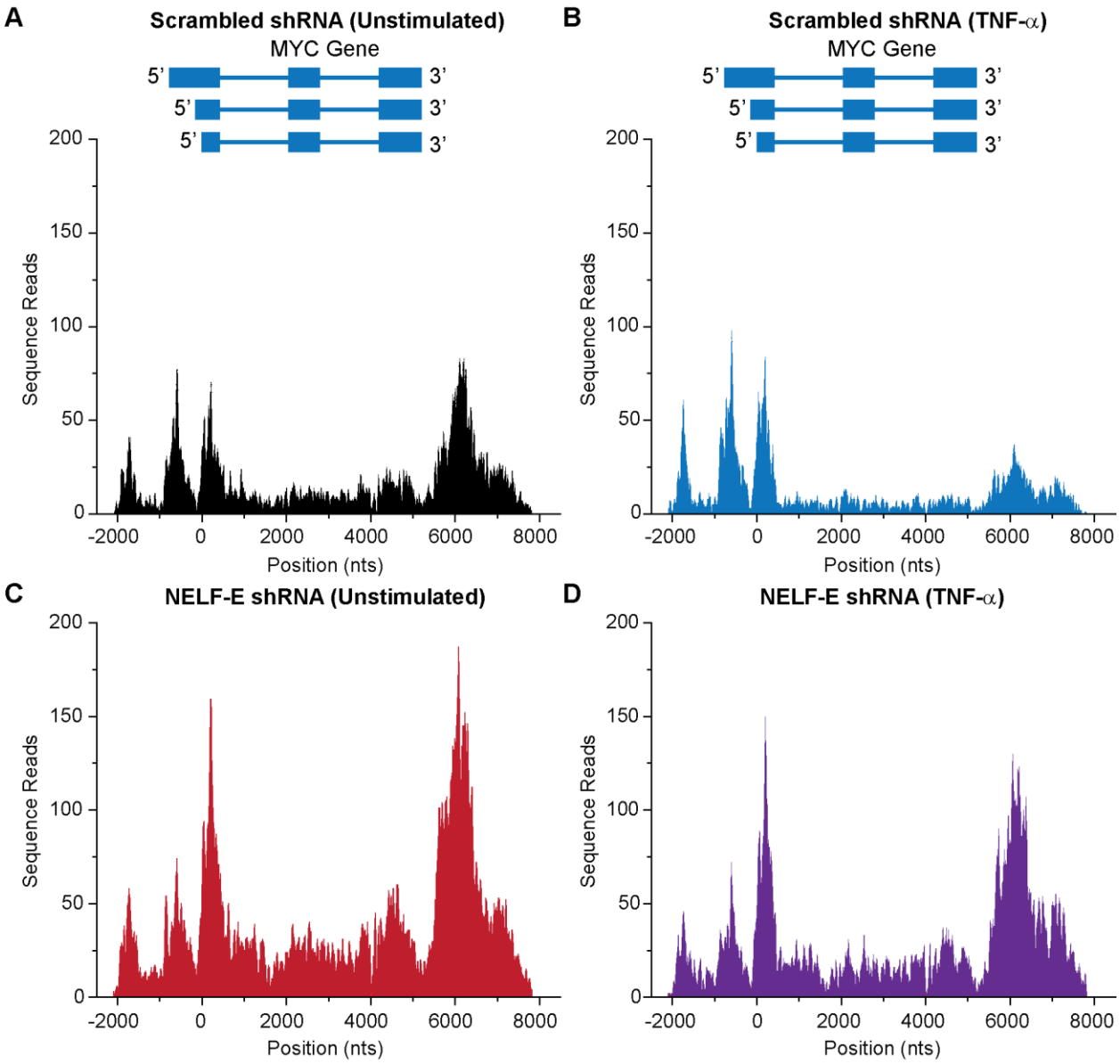

FIG S12 The distribution of RNA polymerase on the MYC Gene was measured by ChIP-Seq assays performed using the parental line E4 and clones carrying the NELF-E shRNA (N1C6) and its scrambled control (N1D9). (A) Unstimulated control (N1D9) cells. (B) Control cells stimulated by 10 ng/ml TNF-α for 60 min. (C) Unstimulated NELF-E shRNA (N1C6) cells. (D) NELF-E shRNA cells activated by 10 ng/ml TNF-α for 60 min. Note that the MYC Gene is an example of a gene that is strongly stimulated by NELF knockdown but slightly down-regulated by TNF-α.

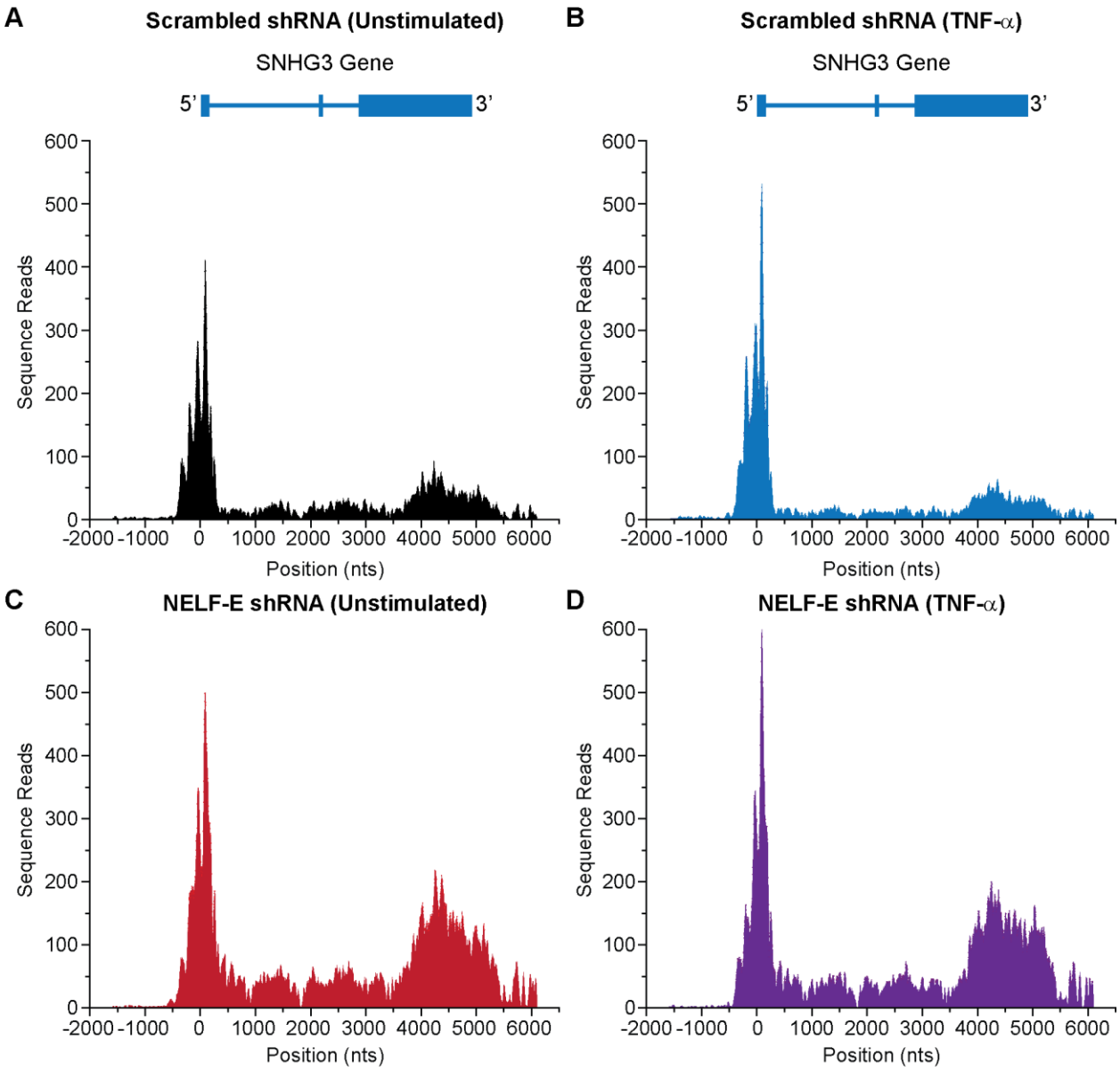

FIG S13 The distribution of RNA polymerase on the SNHG3 Gene was measured by ChIP-Seq assays performed using the parental line E4 and clones carrying the NELF-E shRNA (N1C6) and its scrambled control (N1D9). (A) Unstimulated control (N1D9) cells. (B) Control cells stimulated by 10 ng/ml TNF-α for 60 min. (C) Unstimulated NELF-E shRNA (N1C6) cells. (D) NELF-E shRNA cells activated by 10 ng/ml TNF-α for 60 min. Note that the SNHG3 Gene is an example of a gene that is strongly stimulated by NELF knockdown and weakly responsive to TNF-α.

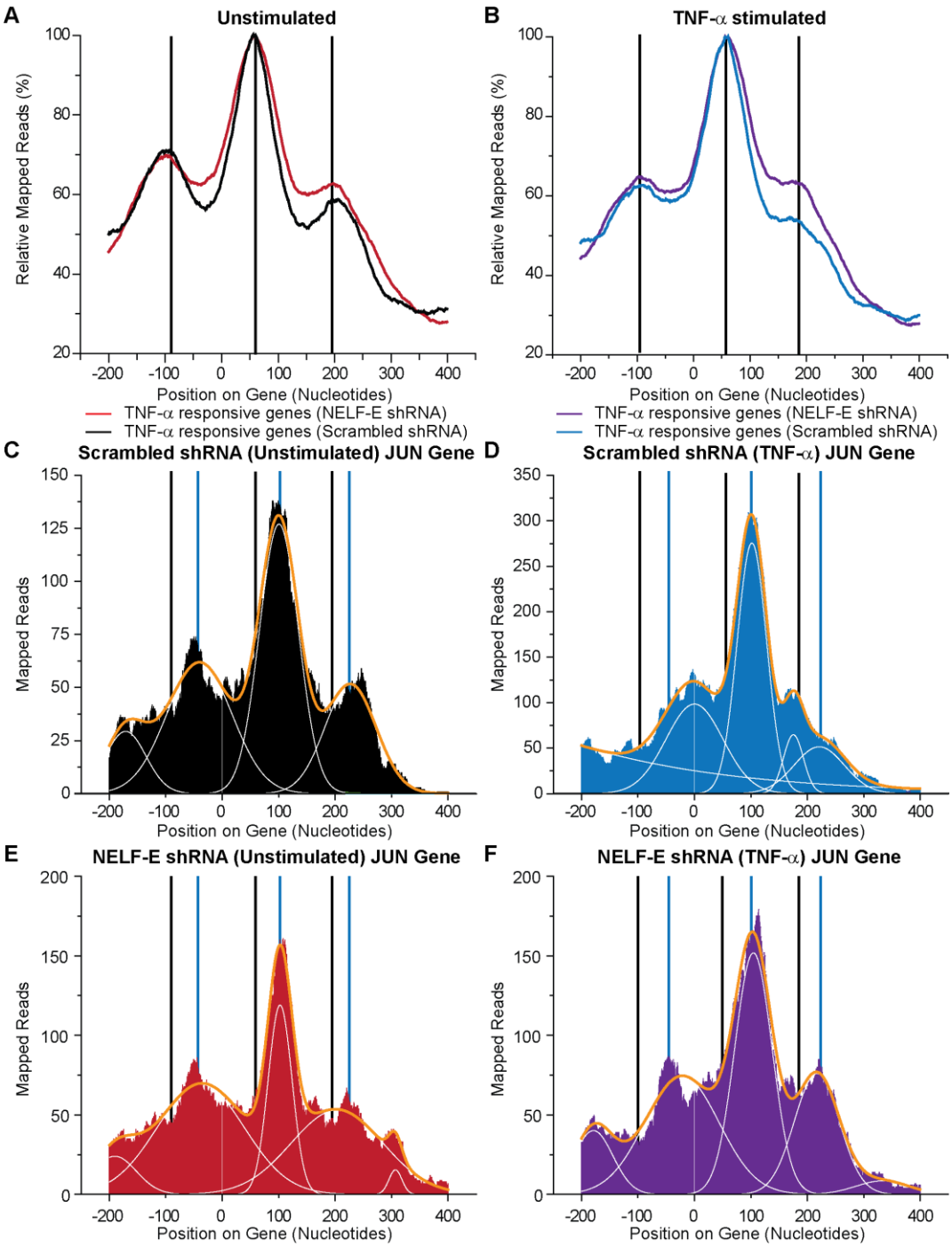

FIG S14 Promoter proximal pause sites on the JUN Gene. Top panels show the average RNAP II distribution relative to the transcription start site for the 500 genes that are most highly activated by TNF-α. (A) Unstimulated control (N1D9) cells. (B) Control cells stimulated by TNF-α. (C) Unstimulated NELF-E shRNA (N1C6) cells. (D) NELF-E shRNA cells stimulated by TNF-α. Black vertical lines indicate the sites of RNAP II the accumulation on averaged cellular genes. Blue vertical lines indicate additional sites of RNAP II accumulation on the HIV LTR. The major peaks were fitted to a series of Gaussian curves (white lines) and summed (yellow lines). Note that NELF knockdown stimulated RNAP II accumulation downstream of +300 but did not shift the location of the major pause sites.

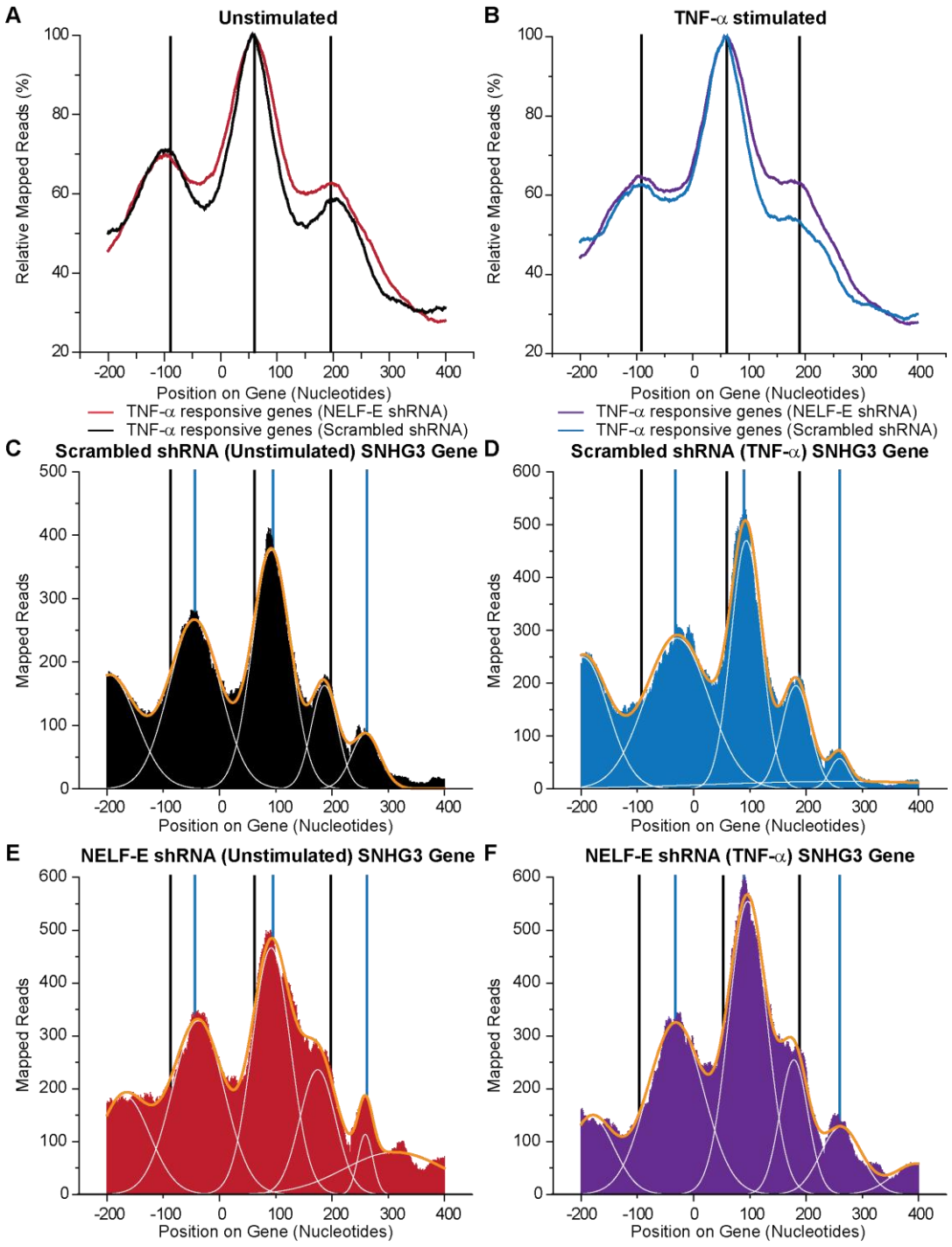

FIG S15 Promoter proximal pause sites on the SNHG3 HIV LTR. Top panels show the average RNAP II distribution relative to the transcription start site for the 500 genes that are most highly activated by TNF-α. (A) Unstimulated control (N1D9) cells. (B) Control cells stimulated by TNF-α. (C) Unstimulated NELF-E shRNA (N1C6) cells. (D) NELF-E shRNA cells stimulated by TNF-α. Black vertical lines indicate the sites of RNAP II the accumulation on averaged cellular genes. Blue vertical lines indicate additional sites of RNAP II accumulation on the HIV LTR. The major peaks were fitted to a series of Gaussian curves (white lines) and summed (yellow lines). Note that NELF knockdown stimulated RNAP II accumulation downstream of +250 but did not shift the location of the major pause sites.

Supplemental References

Friedman, J., Cho, W.K., Chu, C.K., Keedy, K.S., Archin, N.M., Margolis, D.M., and Karn, J. (2011). Epigenetic silencing of HIV-1 by the Histone H3 lysine 27 Methyltransferase Enhancer of Zeste 2 (EZH2). J Virol *85*, 9078-9089.

Pearson, R., Kim, Y.K., Hokello, J., Lassen, K., Friedman, J., Tyagi, M., and Karn, J. (2008). Epigenetic silencing of human immunodeficiency virus (HIV) transcription by formation of restrictive chromatin structures at the viral long terminal repeat drives the progressive entry of HIV into latency. J Virol *82*, 12291-12303.

Wires, E.S., Alvarez, D., Dobrowolski, C., Wang, Y., Morales, M., Karn, J., and Harvey, B.K. (2012). Methamphetamine activates nuclear factor kappa-light-chain-enhancer of activated B cells (NF-kappaB) and induces human immunodeficiency virus (HIV) transcription in human microglial cells. J Neurovirol *18*, 400-410.